


# Accurate measurement of nanomechanical motion in a fiber-taper nano-optomechanical system

Cite as: Appl. Phys. Lett. **115**, 013104 (2019); <https://doi.org/10.1063/1.5110272>

Submitted: 15 May 2019 . Accepted: 18 June 2019 . Published Online: 02 July 2019

Huadan Zheng, Weiqia Qiu, Xiaohang Gu, Yu Zhang, Wenguo Zhu, Bincheng Huang, Huihui Lu, Heyuan Guan, Yi Xiao, Yongchun Zhong, Junbin Fang, Yunhan Luo, Jun Zhang, Jianhui Yu , Frank Tittel, and Zhe Chen



View Online



Export Citation



CrossMark

## ARTICLES YOU MAY BE INTERESTED IN

[Layer-selective spin amplification in size-modulated quantum nanocolumn](#)

Applied Physics Letters **115**, 013102 (2019); <https://doi.org/10.1063/1.5098110>

[Bright electroluminescence in ambient conditions from WSe<sub>2</sub> p-n diodes using pulsed injection](#)

Applied Physics Letters **115**, 011103 (2019); <https://doi.org/10.1063/1.5100306>

[Bloch surface wave ring resonator based on porous silicon](#)

Applied Physics Letters **115**, 011101 (2019); <https://doi.org/10.1063/1.5093435>



### Sensors, Controllers, Monitors

from the world leader in cryogenic thermometry



# Accurate measurement of nanomechanical motion in a fiber-taper nano-optomechanical system

Cite as: Appl. Phys. Lett. **115**, 013104 (2019); doi: [10.1063/1.5110272](https://doi.org/10.1063/1.5110272)

Submitted: 15 May 2019 · Accepted: 18 June 2019 ·

Published Online: 2 July 2019



View Online



Export Citation



CrossMark

Huadan Zheng,<sup>1,2,3</sup> Weiqia Qiu,<sup>2</sup> Xiaohang Gu,<sup>3</sup> Yu Zhang,<sup>3</sup> Wenguo Zhu,<sup>1,3,a)</sup> Bincheng Huang,<sup>2</sup> Huihui Lu,<sup>1,2</sup> Heyuan Guan,<sup>1,2</sup> Yi Xiao,<sup>1,2</sup> Yongchun Zhong,<sup>1,2</sup> Junbin Fang,<sup>3</sup> Yunhan Luo,<sup>3</sup> Jun Zhang,<sup>1,2</sup> Jianhui Yu,<sup>1,2,b)</sup> Frank Tittel,<sup>4</sup> and Zhe Chen<sup>1,2,3</sup>

## AFFILIATIONS

<sup>1</sup>Guangdong Provincial Key Laboratory of Optical Fiber Sensing and Communications, Jinan University, Guangzhou 510632, China

<sup>2</sup>Key Laboratory of Optoelectronic Information and Sensing Technologies of Guangdong Higher Education Institutes, Jinan University, Guangzhou 510632, China

<sup>3</sup>Guangdong Provincial Engineering Technology Research Center on Visible Light Communication and the Guangzhou Municipal Key Laboratory of Engineering Technology on Visible Light Communication, Jinan University, Guangzhou 510632, China

<sup>4</sup>Department of Electrical and Computer Engineering, Rice University, Houston, Texas 77005, USA

a)zhuwg22@163.com

b)Author to whom correspondence should be addressed: [kensomyu@gmail.com](mailto:kensomyu@gmail.com)

## ABSTRACT

The hybrid systems that couple optical and mechanical degrees of freedom in nanoscale devices offer an unprecedented opportunity and development in laboratories worldwide. A nano-optomechanical (NOM) system that converts energy directly/inversely between optics and mechanics opens an approach to control the behavior of light and light-driven mechanics. An accurate measurement of the mechanical motion of a fiber-taper NOM system is a critical challenge. In this work, an optical microscope was used to measure the nanoscale mechanical motion of the fiber taper by introducing white light interference. The resolution of mechanical motion monitoring achieved 0.356 nm with an optomechanical efficiency of  $>20 \text{ nm}/\mu\text{W}$ . This paper describes an approach to characterize NOM transducers between optical and mechanical signals in both classical and quantum fields.

Published under license by AIP Publishing. <https://doi.org/10.1063/1.5110272>

A nano-optomechanical (NOM) system offers an unprecedented opportunity and development in laboratories worldwide. Optomechanical effects in a nanostructure provide new, alternative opportunities to achieve efficient nanophotonic devices without nonlinear crystals, inscrutable waveguides, and optofluidic circuitry.<sup>1</sup> The advantage of a NOM system is that the optomechanical effects become more substantial at the nanoscale making innovative applications feasible, such as the detection of gravitational waves.<sup>2,3</sup> Optical force, which was induced by an optical momentum exchange between light and matter, plays a key role in a NOM system. The optical gradient force, which arises from near field effects,<sup>4</sup> acts transversely to the light propagation direction and increases by orders of magnitude in evanescent coupled waveguides.<sup>5</sup> The increase can be attributed to a greatly enhanced gradient in the near field.<sup>6</sup>

Micro-/nanofiber (MNF) has advantages such as nanosize, excellent flexibility, and strong evanescent field.<sup>7</sup> The MNF has been used

in the research of fundamental physical problems,<sup>8</sup> such as the Abraham-Minkowski dilemma<sup>9–12</sup> and the application of an optical force.<sup>13</sup> In previous research, the light-driven mechanical motion of MNF was phenomenally observed by microscopy but could not be measured accurately and quantitatively. Since the optical momentum exchange caused by an optical force of a few femtonewtons was weak, it is critical to measure the motion of the MNF in the investigation of optical momentum and optical force.

Conventional methods reported to measure nanoscale motion include a position sensitive detector (PSD),<sup>14</sup> a linear variable differential transformer (LVDT),<sup>15</sup> and fiber Bragg grating sensors (FBGs). A PSD requires complicated electronic circuits, and its resolution only reaches the microscale. LVDT is relatively large in physical size and heavy in weight. A FBG sensor must be mounted on the target and is not suitable for noncontact measurements in a NOM system.

In this paper, a fiber-taper NOM system was constructed based on a MNF and a glass substrate (GS). The nanomechanical motion measurement system consists of a microscope and a white light source, which was designed, fabricated, and demonstrated. Due to the interference between the MNF and the GS, the change of the gap distance between the MNF and GS leads to a shift of the interference pattern. The relationship of the pattern shift and the MNF mechanical motion was investigated in detail. The developed nanomechanical motion measurement system was calibrated with a NOM system pumped with different optical power levels. The accuracy and long term stability of the nanomechanical motion measurement system were also evaluated.

The schematic diagram of the experimental system is shown in Fig. 1(a), where  $\theta$  is the tilted angle between MNF and GS and  $g_z$  is the gap between the MNF and the GS. The variation of the gap can be described as the function  $g(z) = g_0 + z \tan \theta$ , where  $g_0$  is the initial gap between the MNF and the GS at  $z = 0$ . The optical field  $\vec{E}_{in}$  with a wavelength range of 300–750 nm illuminates the MNF and GS from the top.  $\vec{E}_{r1}$  and  $\vec{E}_{r2}$  will be reflected from the top surfaces of the MNF and the GS, respectively. The pattern intensity  $I_r(z, \lambda)$  induced by the interference of  $\vec{E}_{r1}$  and  $\vec{E}_{r2}$  can be written as

$$I_r(z, \lambda) = \frac{1}{2} \epsilon_0 c \left\{ E_{r1}^2 + E_{r2}^2 + 2E_{r1}E_{r2} \cos \left[ \frac{4\pi}{\lambda} (g_0 + z \tan \theta) + \frac{4\pi}{\lambda} nd + (\alpha_1 + \alpha_2) \right] \right\}, \quad (1)$$

where  $n$  and  $d$  are the refractive index and diameter of the MNF, respectively.  $\alpha_1$  and  $\alpha_2$  are the additional phases induced by the reflection from the MNF and the GS, respectively. The intensity varies sinusoidally along the  $z$  direction with a spatial period  $T_z = \lambda / (2 \tan \theta)$ . The interference pattern shift  $\Delta L$  in the  $z$  positive direction can be described by  $\Delta L = -\Delta g / \tan \theta$ . The minus sign indicates a pattern shift in a positive direction of  $z$ . As a result, the mechanical motion of MNF leading to the gap change on a nanometer scale can be measured by the pattern shift with an optical microscope.

The experimental setup is shown in Fig. 1(b). The used tapered fiber was fabricated by stripping off its coating of an  $\sim 3$  cm section of single-mode fiber (SMF). The stripped section of the SMF was suspended by fixing its two sides on two translational stages. The suspended section was heated by a flame and was elongated by moving the two stages in the opposite direction until tapered fiber reaches a diameter of  $< 1 \mu\text{m}$ . The MNF is fixed by means of an UV-cured adhesive on a U-shape holder. A wedge GS driven by a piezoelectric

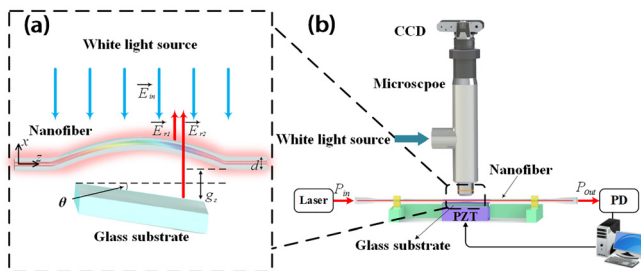


FIG. 1. (a) Principle of white light interferometry; (b) the nanomechanical motion measurement system for NOM motion measurements.

transducer (PZT) was positioned under the MNF with a tilted angle  $\theta$ . The gap between the MNF and the GS can be changed by the PZT with increments of 1 nm. A 1458 nm laser with a maximum power of 300 mW was used as a pump light source to drive the MNF in order to generate an evanescent field induced displacement. The output  $P_{out}$  of the MNF was monitored using a photodetector (PD). A white light source with an emitting wavelength range of 300–750 nm was used to illuminate the MNF. A microscope with a  $20\times$  objective (numerical aperture = 0.4) and a 16 bit-color charge-coupled device (CCD) are used to record the shift of the color pattern on the MNF. The peak of the GS is adjusted below the middle of the suspended MNF using a three-dimensional translational stage. The initial gap  $g_0$  between the MNF and GS can be finely adjusted to  $\sim 1.7 \mu\text{m}$  until the color pattern was observed by a CCD. The PZT and the GS were mounted on an angle adjuster capable of a precision of  $0.001^\circ$ .

The microscopic image taken by the CCD is shown in Fig. 2. The interaction length of the MNF is  $\sim 55 \mu\text{m}$ . The diameter of the MNF was measured to be  $0.86 \mu\text{m}$ . To obtain the linear relationship between a shift  $\Delta L$  and a gap change  $\Delta g$ , the GS is precisely moved close to the MNF by a PZT, leading to a corresponding decrease in the gap size. The tilted angle  $\theta$  is set to  $0.3^\circ$ . The microscopic images of the color pattern for  $\Delta g$  are shown in Figs. 2(a)–2(e). The red, green, and blue (RGB) components of the color pattern along the MNF are extracted from Figs. 2(a)–2(e) and correspondingly shown in Figs. 2(f)–2(j). The pattern shift  $\Delta L$  can be measured by tracing the peaks of the RGB distribution as indicated by red arrows in Figs. 2(a)–2(e) and Figs. 2(f)–2(j). In the experiment, the green component is regarded as the reference beam due to its highest intensity and signal-to-noise ratio. As a result, the color pattern will shift along the  $z$  direction as the gap decreases.

The relationship between the shift  $\Delta L$  and the gap change  $\Delta g$  was verified for various tilted angles  $\theta$ . The linear fitting of three groups of

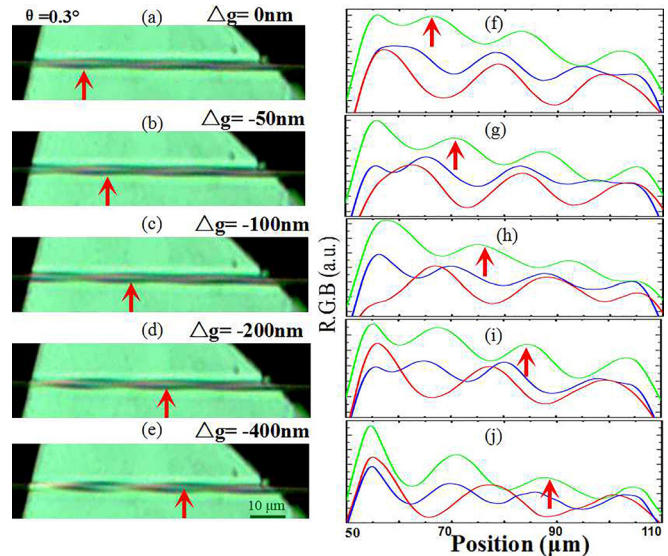


FIG. 2. (a)–(e) Microscopic images of the color pattern for  $\Delta g = 0$  nm,  $-50$  nm,  $-100$  nm,  $-200$  nm, and  $-400$  nm, respectively. (f)–(j) The RGB component distribution along the MNF for  $\Delta g = 0$  nm is  $-50$  nm,  $-100$  nm,  $-200$  nm, and  $-400$  nm, respectively.

$\Delta g$  as a function of  $\Delta L$  is shown in Fig. 3. According to Eq. (2), the tilted angles are calculated to be  $0.3^\circ$ ,  $0.4^\circ$ , and  $0.8^\circ$ . The  $R^2$  values for  $\theta = 0.3^\circ$ ,  $0.4^\circ$ , and  $0.8^\circ$  are 0.997, 0.999, and 0.998, respectively, indicating a good linearity. The slopes of the three curves show that the sensitivity of the system is  $2.469 \mu\text{m}/\text{nm}$ ,  $1.879 \mu\text{m}/\text{nm}$ , and  $0.724 \mu\text{m}/\text{nm}$ , respectively. Since the minimum resolvable distance of the microscope with an objective lens of a NA = 0.4 is  $\sim 0.9 \mu\text{m}$ , the estimated optimum resolution of displacement is  $0.365 \text{ nm}$  according to Abbe's limit.

To verify the measurement of the mechanical motion induced by the NOM system, a pump laser with a wavelength of  $1458 \text{ nm}$  was coupled into the MNF. The pump light propagated along the MNF and the optical energy was evanescently coupled into the GS, leading to a momentum exchange between the MNF and the GS. Subsequently, repulsive optical force exerted on the MNF and pushed the MNF away from the GS on a nanoscale. The increase in the gap  $\Delta g$  leads to a shift  $\Delta L$  of the color pattern. Since the effective pump power in the MNF is  $\sim 10^{-6} \text{ W}$ , the contribution of the photothermal effect can be ignored.

To evaluate the optomechanical efficiency of the nanomechanical motion measurement system, the displacements of MNF in the NOM system pumped by different powers were measured. To obtain the exact pump power in the MNF, the optical loss between the pump laser, SMF, and MNF was measured first. Before the fabrication of the MNF, the output power  $P_{01}$  from the SMF was  $3.8 \text{ mW}$  with a pump power of  $5 \text{ mW}$ , corresponding to a fiber coupling efficiency of  $76\%$ . After fabrication of the MNF, the transmitted power of the MNF decreased to  $0.19 \mu\text{W}$  which can be measured by cutting off the MNF in the middle, corresponding to an optical loss of  $42.98 \text{ dB}$ . The output power from the pump laser was set to be  $110 \text{ mW}$ ,  $150 \text{ mW}$ ,  $190 \text{ mW}$ , and  $230 \text{ mW}$  corresponding to  $5.58 \mu\text{W}$ ,  $7.61 \mu\text{W}$ ,  $9.64 \mu\text{W}$ , and  $11.67 \mu\text{W}$  in the MNF, respectively. For each pump power, the laser is turned on and off once with the result that the color pattern moves back and forth. As shown in Fig. 4, the color patterns with and without pump lasers were extracted from a video which was recorded by a CCD.

As shown in Figs. 4(c), 4(d), 4(g), and 4(h), the green component distributions along the MNF were extracted. The dotted lines and solid

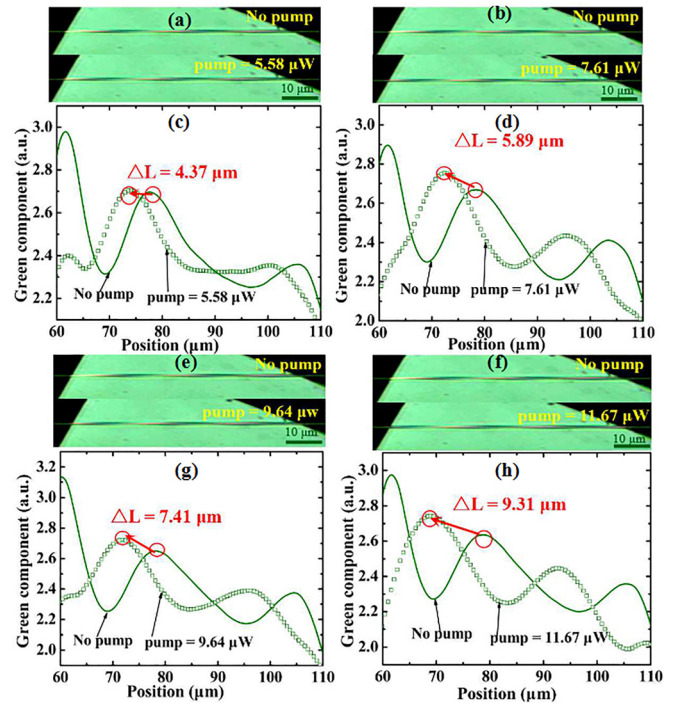


FIG. 4. Microscopic images of the color pattern and the distributions of the green component when four different input pump powers for a tilted angle of  $\theta = 0.3^\circ$ .

lines in Fig. 4 denote the green component distributions without and with pump light, respectively. The measured shifts of the color pattern  $\Delta L$  are  $4.37 \mu\text{m}$ ,  $5.89 \mu\text{m}$ ,  $9.64 \mu\text{m}$ , and  $11.67 \mu\text{m}$  for the pump power at  $5.58 \mu\text{W}$ ,  $7.61 \mu\text{W}$ ,  $9.64 \mu\text{W}$ , and  $11.67 \mu\text{W}$ , respectively. Using a sensitivity of  $2.469 \mu\text{m}/\text{nm}$  for  $\theta = 0.3^\circ$ , the shifts can be converted into the MNF mechanical motion induced by the corresponding evanescent field.

In the case of  $\theta = 0.3^\circ$ ,  $0.4^\circ$ , and  $\theta = 0.8^\circ$ , the linear relationship between MNF mechanical motion and pump power is plotted in Fig. 5. The  $R^2$  values, obtained from Fig. 5(a), for  $\theta = 0.3^\circ$ ,  $0.4^\circ$ , and  $0.8^\circ$  were 98.9%, 98.7%, and 99.1%, respectively, showing a good linear relationship with the pump power. Based on the linear fitting to MNF optomechanical displacements, the optomechanical efficiencies for tilted angles  $\theta = 0.3^\circ$ ,  $0.4^\circ$ , and  $0.8^\circ$  can be obtained and are  $8.19 \text{ nm}/\mu\text{W}$ ,

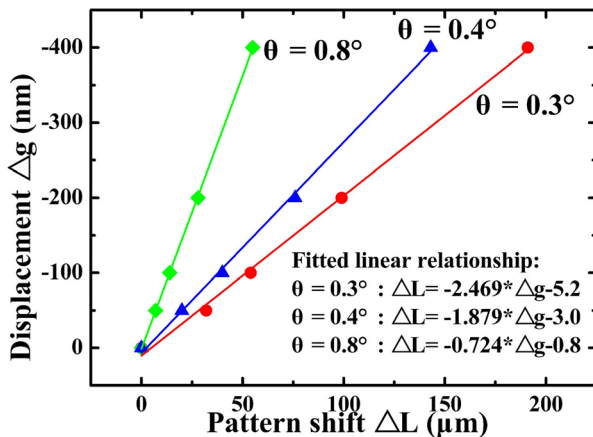


FIG. 3. Linear relationship between  $\Delta g$  and  $\Delta L$  at three tilted angles.

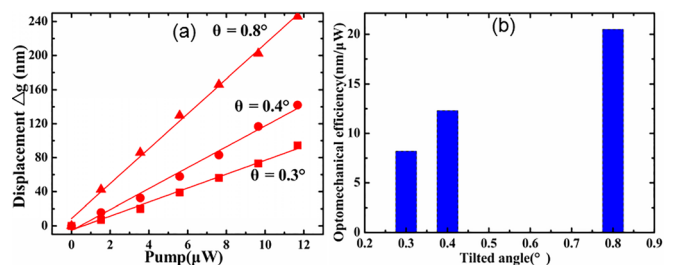
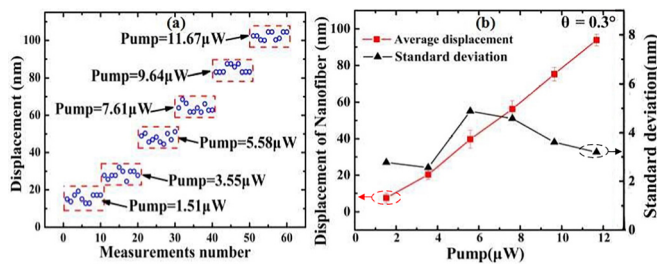


FIG. 5. (a) The measured nano-optomechanical displacements of the MNF with different pump powers at three tilted angles  $\theta = 0.3^\circ$ ,  $0.4^\circ$ , and  $0.8^\circ$ ; (b) optomechanical efficiency of the system at different tilted angles.





**FIG. 6.** (a) Measurements of fiber nano-optomechanical displacements at six different pump powers; (b) variation of standard deviations with pump power.

12.3 nm/ $\mu$ W, and 20.5 nm/ $\mu$ W, respectively. According to Fig. 5(b), the larger tilted angle leads to a higher optomechanical efficiency, which indicates that a stronger repulsive optical force was generated.

In order to obtain the accuracy and stability of the nanomechanical motion measurement system, the fiber taper motion in the NOM system pumped by different laser output powers was repeatedly measured ten times. Figure 6(a) shows the measurements of the fiber nano-optomechanical displacements at pump powers of 1.51  $\mu$ W, 3.55  $\mu$ W, 5.58  $\mu$ W, 7.61  $\mu$ W, 9.64  $\mu$ W, and 11.67  $\mu$ W, respectively. The fluctuations of displacements can be attributed to the fluctuations of both the air and the pump power. As shown in Fig. 6(b), standard deviations for the pump powers of 1.51  $\mu$ W, 3.55  $\mu$ W, 5.58  $\mu$ W, 7.61  $\mu$ W, 9.64  $\mu$ W, and 11.67  $\mu$ W are 2.77 nm, 2.56 nm, 4.88 nm, 4.57 nm, 3.61 nm, and 3.20 nm, respectively. As a result, when the maximum displacement of the fiber reached  $\sim 100$  nm, the standard deviation was  $\sim 3$  nm, corresponding to an error of  $\pm 3\%$ .

In conclusion, a nanomechanical motion measurement system, which consisted of a microscope and a white light source, was demonstrated to be able to measure the light-driven mechanical motion of a micro/nanofiber (MNF) in a fiber-taper nano-optomechanical (NOM) system. The gap distance between the MNF and the GS was accurately measured by the interference pattern shift induced by the MNF and GS surface. The experimental results show that the color pattern has a linearity of  $>99\%$  with the mechanical motion of the MNF. A minimum measurable MNF displacement of 0.356 nm was achieved with a tilted angle of  $0.3^\circ$ . The NOM measurement system is used to measure the mechanical motion of the MNF in a fiber-taper NOM system pumped by a 1458 nm laser. The linearity between the obtained color pattern shift and the MNF mechanical motion for tilted angles of  $0.3^\circ$ ,  $0.4^\circ$ , and  $0.8^\circ$  is 0.997, 0.999, and 0.998, respectively. The optomechanical efficiency of the measurement system increased with different pump power levels. The results show that for a tilted angle  $\theta$  of  $0.8^\circ$ , the optomechanical efficiencies of the measurement system reached up to 20.5 nm/ $\mu$ W. Repetitive experiments show a good accuracy and stability of the measurement system. The proposed mechanical

measurement system can not only provide the nondestructive measurement of nanometric displacement in a NOM system but also provide an alternative ultrasensitive way to sense and measure an ultraweak force.

See the [supplementary material](#) for the pattern shift recorded by the CCD with a pump power of  $P = 7.61 \mu\text{W}$ .

This work is supported by the National Natural Science Foundation of China (Nos. 11004086, 61675092, 61275046, 61475066, 61405075, and 61601404), Natural Science Foundation of Guangdong Province (Nos. 2014A030313377, 2015A030306046, and 2015A030313320), Special Funds for Major Science and Technology Projects of Guangdong Province (Nos. 2014B010120002, 2014B010117002, and 2015B010125007), Project of Guangzhou Industry Leading Talents (No. CXLJTD-201607), Planned Science & Technology Project of Guangzhou (No. 201506010046), Foundation for Distinguished Young Talents in Higher Education of Guangdong (Nos. 2019KQNCX009 and 2018KQNCX279), the Fundamental Research Funds for the Central Universities (No. 21619402), and State Key Laboratory of Applied Optics (SKLAO-201914). Frank Tittel acknowledges the financial support from the US National Science Foundation (NSF) ERC MIRTHER award, a NSF NeTS Large “ASTRO” award (No. R3H685), and a grant C-0586 from the Welch Foundation.

## REFERENCES

- <sup>1</sup>A. S. Shalin, P. Ginzburg, P. A. Belov, Y. S. Kivshar, and A. V. Zayats, *Laser Photonics Rev.* **8**, 131 (2014).
- <sup>2</sup>T. J. Kippenberg and K. J. Vahala, *Science* **321**, 1172 (2008).
- <sup>3</sup>L. Midolo, A. Schliesser, and A. Fiore, *Nat. Nanotechnol.* **13**, 11 (2018).
- <sup>4</sup>M. Eichenfield, R. Camacho, J. Chan, K. J. Vahala, and O. Painter, *Nature* **459**, 550 (2009).
- <sup>5</sup>H. Cai, K. J. Xu, A. Q. Liu, Q. Fang, M. B. Yu, G. Q. Lo, and D. L. Kwong, *Appl. Phys. Lett.* **100**, 013108 (2012).
- <sup>6</sup>M. Li, W. H. P. Pernice, C. Xiong, T. Baehr-Jones, M. Hochberg, and H. X. Tang, *Nature* **456**, 480 (2008).
- <sup>7</sup>L. M. Tong, R. R. Gattass, J. B. Ashcom, S. L. He, J. Y. Lou, M. Y. Shen, I. Maxwell, and E. Mazur, *Nature* **426**, 816 (2003).
- <sup>8</sup>W. L. She, J. H. Yu, and R. H. Feng, *Phys. Rev. Lett.* **101**, 243601 (2008).
- <sup>9</sup>E. A. Hinds and S. M. Barnett, *Phys. Rev. Lett.* **102**, 050403 (2009).
- <sup>10</sup>M. Masud, *Phys. Rev. Lett.* **108**, 193901 (2012).
- <sup>11</sup>M. Khorrami, *Phys. Rev. Lett.* **110**, 089404 (2013).
- <sup>12</sup>J. H. Yu, S. S. Jin, Q. S. Wei, Z. G. Zang, H. H. Lu, X. L. He, Y. H. Luo, J. Y. Tang, J. Zhang, and Z. Chen, *Sci. Rep.* **5**, 7710 (2015).
- <sup>13</sup>J. H. Yu, R. H. Feng, and W. L. She, *Opt. Express* **17**, 4640 (2009).
- <sup>14</sup>E. Liénard, M. Herbane, G. Ban, G. Darius, P. Delahaye, D. Durand, X. Fléchar, M. Labalme, F. Mauger, A. Mery, O. Naviliat-Cuncic, and D. Rodríguez, *Nucl. Instrum. Methods Phys. Res., Sect. A* **551**, 375 (2005).
- <sup>15</sup>S. T. Wu, S. C. Mo, and B. S. Wu, *Sens. Actuators, A* **141**, 558 (2008).